ORNL/NUREG/TM-39



# CORTAP: A Coupled Neutron Kinetics-Heat Transfer Digital Computer Program for the Dynamic Simulation of the High Temperature Gas Cooled Reactor Core

J. C. Cleveland

Prepared for the U.S. Nuclear Regulatory Commission
Office of Nuclear Regulatory Research
Under Interagency Agreement ERDA 40-551-75

OAK RIDGE NATIONAL LABORATORY
OPERATED BY UNION CARBIDE CORPORATION FOR THE ENERGY RESEARCH AND DEVELOPMENT ADMINISTRATION

BLANK PAGE

Printed in the United States of America Available from
National Technical Information Service
U S Department of Commerce
5285 Port Royal Road Springfield Virginia 22161
Price Printed Copy $4 50 Microfiche $3 00

ORNL/NUREG/TM-39
Dist. Category NRC-8

Contract No. W-7405-eng-26

Engineering Technology Division

# CORTAP: A COUPLED NEUTRON KINETICS-HEAT TRANSFER DIGITAL COMPUTER PROGRAM FOR THE DYNAMIC SIMULATION OF THE HIGH TEMPERATURE GAS COOLED REACTOR CORE

J. C. Cleveland

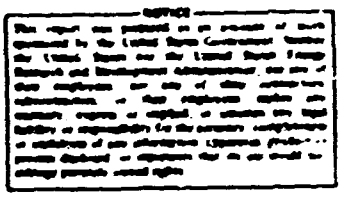

Manuscript Completed - January 7, 1977
Date Published - January 1977

NOTICE: This document contains information of a preliminary nature. It is subject to revision or correction and therefore does not represent a final report.

Prepared for the
U.S. Nuclear Regulatory Commission
Office of Nuclear Regulatory Research
Under Interagency Agreement ERDA 40-551-75

Prepared by the
OAK RIDGE NATIONAL LABORATORY
Oak Ridge, Tennessee 37830
operated by
UNION CARBIDE CORPORATION
for the
ENERGY RESEARCH AND DEVELOPMENT ADMINISTRATION

## CONTENTS

## ABSTRACT

CORTAP (Core Transient Analysis Program) was developed to predict the dynamic behavior of the High Temperature Gas Cooled Reactor (HTGR) core under normal operational transients and postulated accident conditions. CORTAP is used both as a stand-alone component simulation and as part of the HTGR nuclear steam supply (NSS) system simulation code ORTAP. The core thermal neutronic response is determined by solving the heat transfer equations for the fuel, moderator and coolant in an average powered region of the reactor core. The space independent neutron kinetics equations are coupled to the heat transfer equations through a rapidly converging iterative technique. The code has the capability to determine conservative fuel, moderator and coolant temperatures in the "hot" fuel region. For transients involving a reactor trip, the core heat generation rate is determined from an expression for decay heat following a scram. Nonlinear effects introduced by temperature dependent fuel, moderator and coolant properties are included in the model.

CORTAP predictions will be compared with dynamic test results obtained from the Fort St. Vrain reactor owned by Public Service of Colorado, and, based on these comparisons, appropriate improvements will be made in CORTAP.

Keywords: gas cooled reactors, dynamic response, programs (computer), neutron kinetics, reactor core.

## NOMENCLATURE

$A$ - area

$\underline{A}$ - coefficient matrix

$\alpha$ - temperature coefficient of reactivity

$\beta$ - delayed neutron fraction

$c_p$ - specific heat of solid

$c_{p,He}$ - specific heat of helium

$C$ - conductance (in heat transfer equation); delayed neutron precursor concentration (in neutron kinetics equations)

$C'$ - conductance accounting for combination of conductances in series

$D$ - hydraulic diameter

$\epsilon$ - convergence criteria

$f^z$ - axial peaking factor

$G$ - mass flux

$h$ - heat transfer coefficient

$\underline{I}$ - unit matrix

$k$ - conductivity (in heat transfer equations); or neutron multiplication factor (in neutron kinetics equations)

$\ell$ - average neutron lifetime from release to loss

$m$ - mass

$M_c$ - heat capacity

$n$ - neutron density

$N$ - number of neutron kinetics time steps per heat transfer time step

$Q$ - heat generation rate density

$Re$ - Reynold's number

$R_p$ - radius of fuel stick

BLANK PAGE

$R_M$ - radius of graphite moderator in unit cell

$\rho$ - density (in heat transfer equations); or reactivity (in neutron kinetics equations)

r - distance measured from fuel stick centerline

s - distance measured from fuel stick centerline to outer surface of a node

t - time

$\Delta t$ - time step

T - temperature

$\vec{T}$ - vector of nodal temperatures

$\mu$ - viscosity

V - volume

W - flow rate

$\vec{Z}$ - forcing function vector

Superscripts:

a - axial

F - fuel stick

LR - lower reflector

M - moderator

r - radial

R - reflector

UR - upper reflector

Subscripts:

b - bulk coolant

$\ell$ - centerline

F - fuel

G - graphite

gas - denotes gas temperature used in determining heat flow rate from moderator

HT - denotes heat transfer time step

IM - inner surface of moderator

IN - inlet to node

INLET - inlet to core

i - radial nodal index (in heat transfer equations); or delayed neutron group number (in neutron kinetics equations)

I - outermost radial node in moderator

j - axial nodal index

J - lowest axial node in active fuel section of unit cell

M - moderator

NK - denotes neutron kinetics time step

NUR - number of axial nodes representing upper reflector

NLR - number of axial nodes representing lower reflector

OUT - outlet

o - denotes value of variable at time = 0.0

Ref - reference value

S - solid

# 1. INTRODUCTION

CORTAP simulates the core thermal and neutronic response of the HTGR to normal operational transients and to postulated accident conditions. This response is determined by coupling the neutron kinetics equations to the heat transfer equations for the fuel, moderator and coolant in an averaged powered region of the reactor core. The model represents a unit cell consisting of a fuel stick, the surrounding graphite moderator and coolant channels in the averaged powered region. The code also has the capability to determine conservative values of fuel, moderator and coolant temperatures in the "hot" fuel region.

The present version of CORTAP has the following features:

a) Up to 60 nodes may be used to represent an average or "hot" fuel stick, the surrounding graphite and coolant channels the top and bottom reflector elements and the core support block. The model includes the temperature dependence of the fuel and moderator conductivity, density and specific heat and the helium transport properties. Therefore up to 60 first order, nonlinear, inhomogeneous differential equations are used to represent the core thermal response.

b) Heat transfer from the graphite to the coolant is calculated based on the helium flow regime (turbulent-transitional-laminar).

c) The neutron kinetics behavior of the core is modeled using the space independent neutron kinetics equations with six groups of delayed neutrons. The "prompt jump" approximation is not made.

BLANK PAGE

d) Fuel and moderator temperature coefficients of reactivity are considered to be temperature dependent.

e) The neutron kinetics equations are coupled to the heat transfer equations through a rapidly converging iterative technique so that correct fuel and graphite temperatures are used in determining the feedback reactivity rather than temperatures existing at the end of a previous time step.

f) A smaller computational time step is used for the solution of the neutron kinetics equations than is used for the solution of the heat transfer equations since the response of the reactor power to reactivity changes is much faster than the response of fuel and moderator temperatures to changes in core power.

g) For transients involving a reactor trip the core heat generation rate is determined from an expression for power decay following a scram.

h) Input to the code includes the coolant flow rate and inlet temperature as functions of time. Axial relative power peaking factors are input and assumed constant during transients. The time dependence of the component of the reactivity change due to control rod motion must also be input.

CORTAP was developed both as an aid in the evaluation of the General Atomic system transient analysis code TAP[1] and as an independent method of analyzing transients affecting the HTGR core.

This report contains a description of the HTGR core, the techniques used in the CORTAP simulation, comparisons of CORTAP results with results

obtained by General Atomic, input instructions and sample input. A deck and a listing of the code are available upon request.

## 2. DESCRIPTION OF THE HTGR CORE

The Fort St. Vrain (FSV) hexagonal fuel elements and their arrangement within the reactor core are shown in Figs. 2.1 through 2.4. The FSV core design is quite similar to the large HTGR core design. Each hexagonal element (Fig. 2.1), which is ~14 in. across the flats and ~31 in. high, consists of fuel sticks, containing bonded coated fuel particles, and coolant channels. During reactor operation helium flows downward through the channels.

The arrangement of the hexagonal elements in the FSV core is shown in Fig. 2.3. A stack of six layers of fuel elements with seven hexagonal fuel elements in each layer is referred to as a refueling region. The central hexagonal element in each layer is a control rod element (Fig. 2.2) which contains two control rod channels and a channel for the reserve shutdown spheres. Reflector elements are located both above and below each active fuel column as well as around the circumference of the active core. The core is supported on support blocks (Fig. 2.3) which rest on core support posts located in the lower core plenum.

The inlet to each refueling region contains an adjustable orifice which is used to control the coolant flow to the refueling region so that the power to flow ratios for all refueling regions are essentially equal. The orifice is positioned based on the value of each refueling region's outlet gas temperature, which is monitored by thermocouples located in the core support block. The fact that the coolant flow to

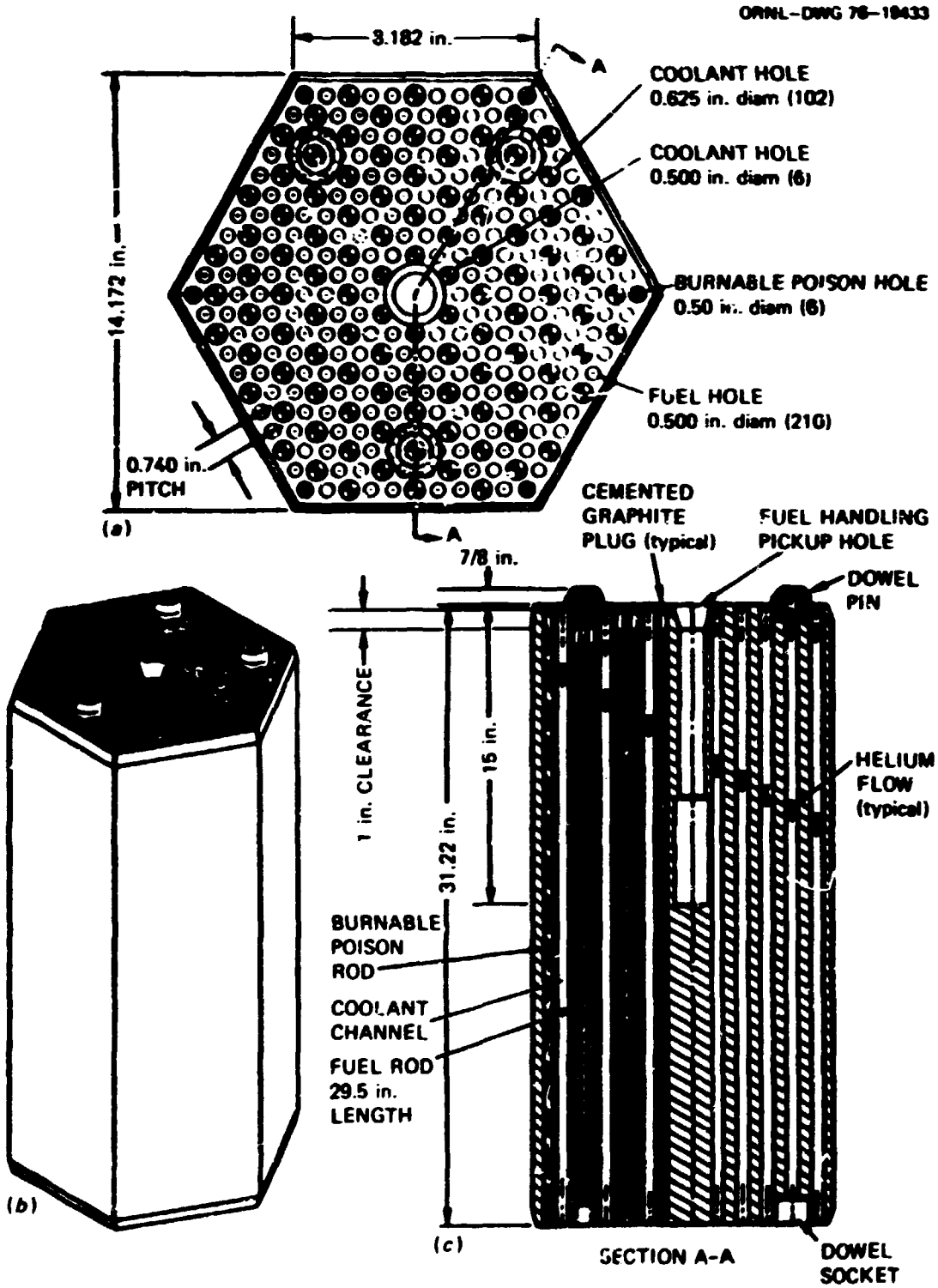


Fig. 2.1. HTGR fuel element, Fort St. Vrain reactor.

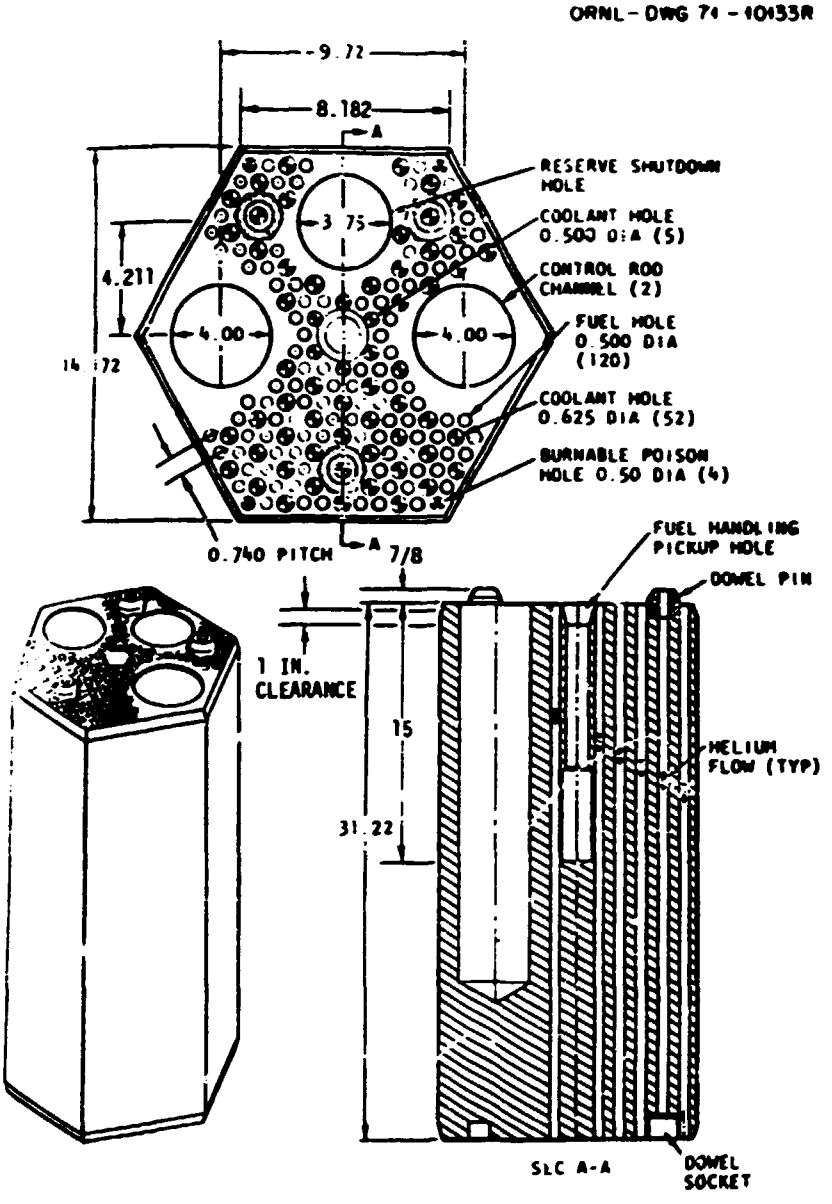


Fig. 2.2. HTGR fuel element, showing holes for control rods. Design for the Fort St. Vrain reactor by the General Atomic Company; similar designs are proposed for larger plants.

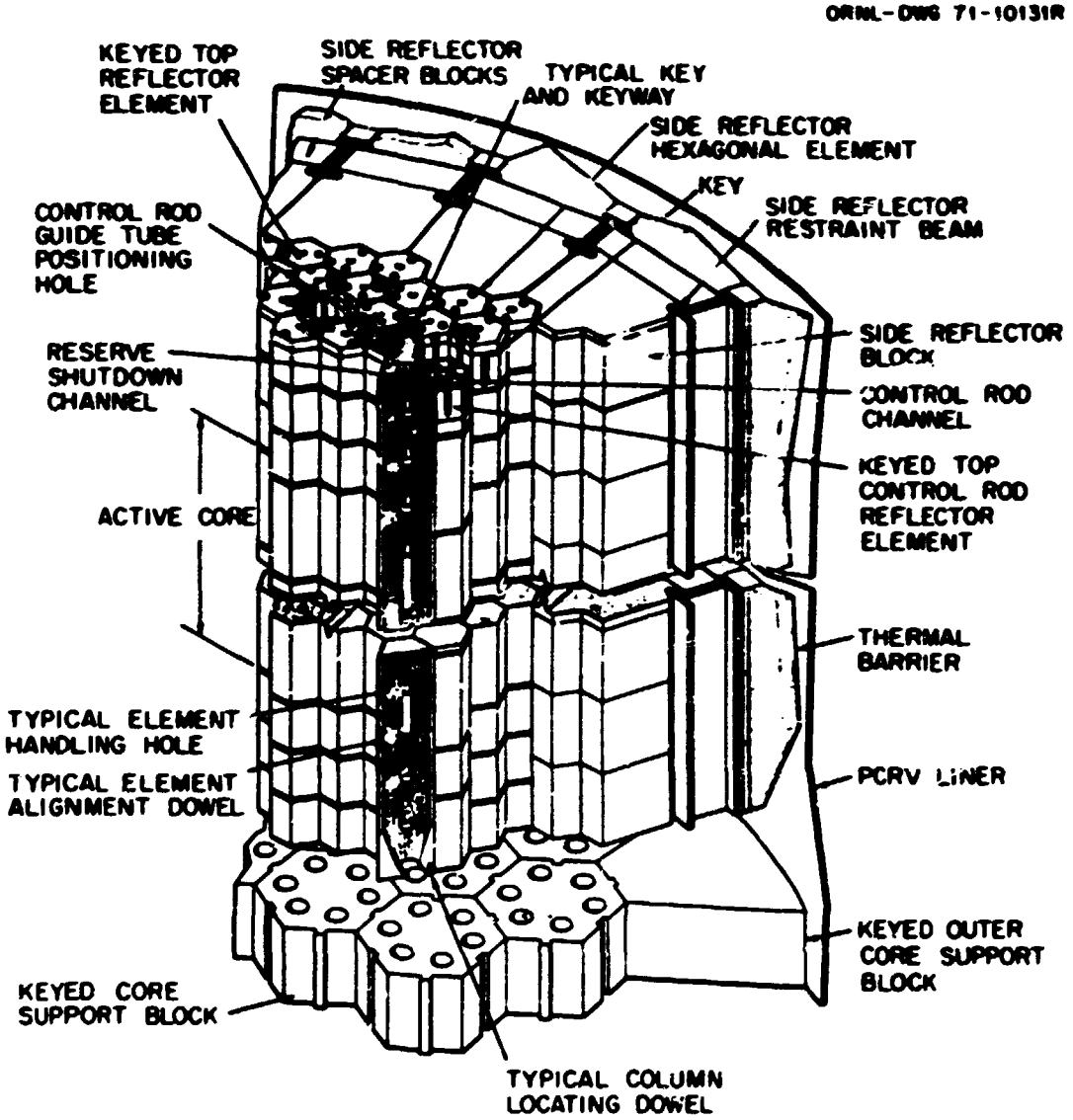


Fig. 2.3. Core block arrangement for the Fort St. Vrain HTGR.

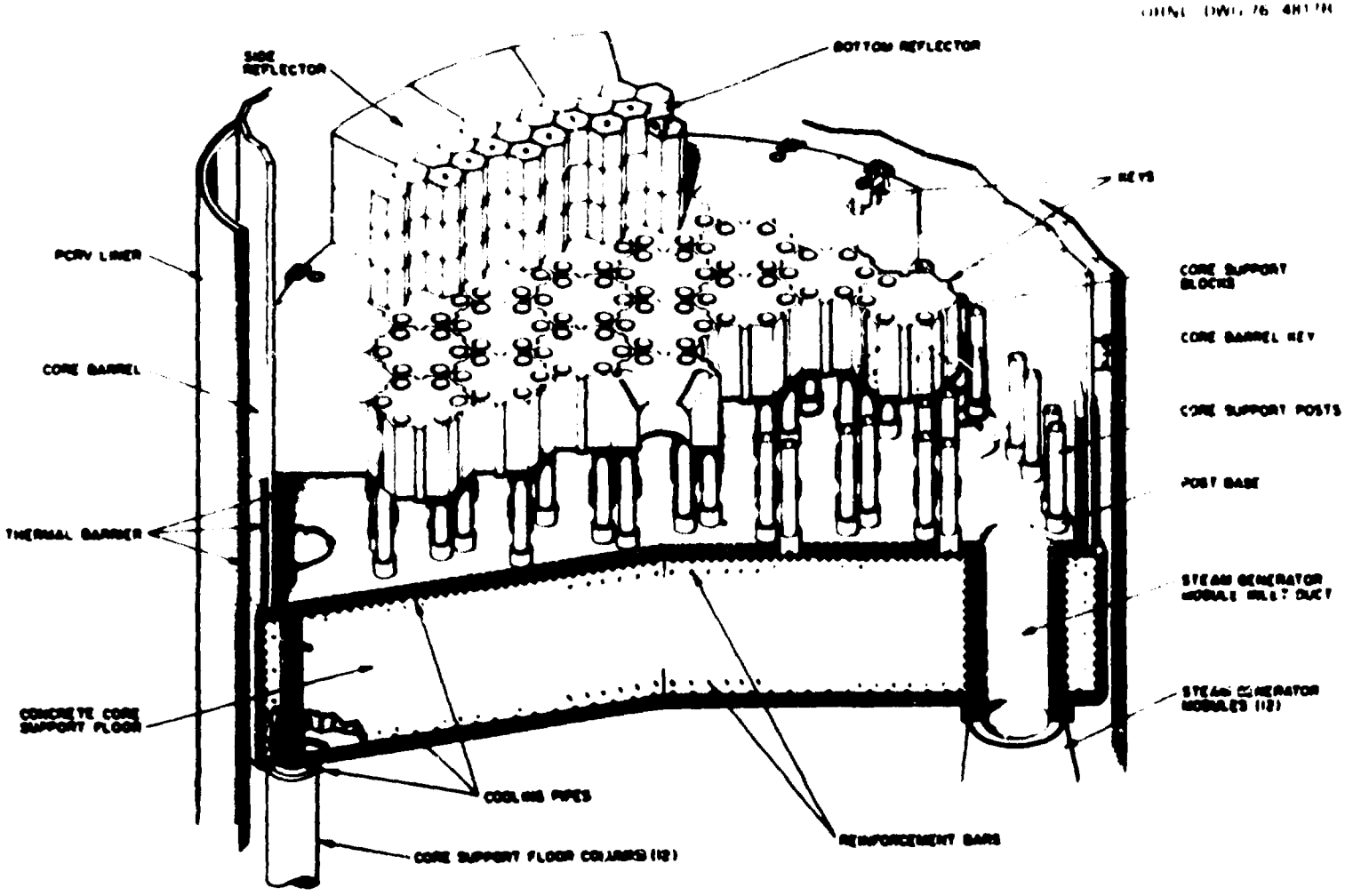


Fig. 2.4 Lower plenum arrangement.

each refueling region is controlled by orifices and is directed through channels simplifies HTGR core modeling compared to LWR core modeling especially in the calculation of peak fuel temperatures since the uncertainties in predicting the coolant flow to the "hot" region should be less for the HTGR.

## 3. MODEL DEVELOPMENT

### 3.1 Active Core Heat Transfer Model

As can be seen in Fig. 2.1, except for the deviations around the fuel handling pickup hole and near the edge of the element, the regular hexagonal elements are composed of an array of triangular cells as shown in Fig. 3.1-a. For conditions in which there is sufficient coolant flow so that the heat flow between a refueling region and adjacent regions is negligible compared to the heat removed by the coolant through forced convection, the three lateral surfaces of the triangular element shown in Fig. 3.1-a (and actually the surfaces of the smaller element bounded by the dotted lines) can be modeled as surfaces of zero heat flux. If this approximation of an adiabatic cell is made when determining peak fuel temperatures, conservative results are obtained since in reality heat flow to adjacent regions would be away from the hot region.

For the coupled neutron kinetics-heat transfer calculations, CORTAP determines the fuel and moderator temperatures and the axial coolant temperature within a triangular unit cell containing an average fuel stick; i.e., a fuel stick with a radial relative power density factor of 1.0. The temperature feedback components of the core reactivity are

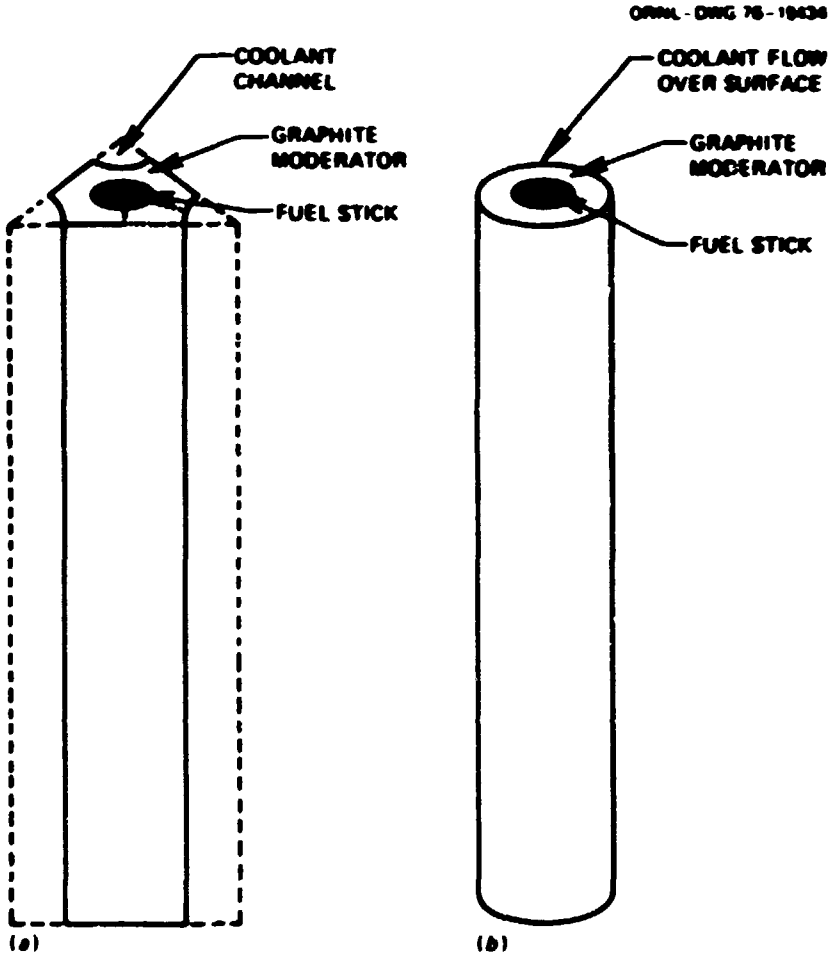


Fig. 3.1. (a) Triangular symmetry element in HTGR fuel block; (b) equivalent cylindrical unit cell.

determined based on changes in the average fuel and graphite temperatures within this unit cell.

The deviation of the fuel stick and coolant channel geometry from a repetitive pattern of triangular cells near the edges of the hexagonal elements and near the control rod and reserve absorber channels results in a fuel to moderator volume ratio in the triangular cell that is greater than the fuel to moderator volume ratio on a refueling region basis.[2] To account for this difference, the density of the graphite in the unit cell is appropriately increased during long term transients to correctly depict the heat capacity effects of the graphite. This modification does not change the steady-state temperature distribution within the fuel and moderator. For short term transients lasting no more than approximately 20 minutes, this modification is not made thus resulting in conservative predictions of fuel and graphite temperatures.

For calculational purposes it is convenient to convert the triangular cell (Fig. 3.1-a) to an equivalent cylindrical cell shown in Fig. 3.1-b. This equivalent cell consists of a fuel stick surrounded by an annular ring of graphite which is cooled on the surface by helium flow. The heat conduction equations can then be solved in two-dimensional (r-z) geometry rather than three-dimensional geometry. To ensure that the equivalent cell representation adequately models the dynamic response of the triangular element the following modeling techniques are used:

a) The volume of the moderator in the triangular element is conserved in the cylindrical cell due to the importance of the graphite heat capacity in transient calculations.

b) The film heat transfer coefficient is modified by the ratio of the actual moderator to coolant heat transfer area in the triangular element to the moderator to coolant heat transfer area in the cylindrical cell since the actual heat transfer area is not conserved in transforming to the cylindrical cell.

c) A detailed steady-state temperature distribution is obtained for the triangular element outlined by the dotted lines in Fig. 3.1-a. This is done with the ORNL general heat conduction code HEATING3[3] using approximately 400 nodal points for the simulation.

d) The results of this calculation of the detailed temperature distribution within the triangular cell are compared with results of a calculation using the cylindrical model. The moderator conductance in the cylindrical model is then modified by a "shape factor" to account for the change from the moderator's actual geometry. This "shape factor" forces the temperature drop across the moderator as calculated by the cylindrical model to agree with the difference between the average moderator temperatures at the surface of the fuel hole and the coolant hole respectively as calculated by HEATING3. Table 3.1 shows an example of the agreement obtained between the triangular and cylindrical representations for steady-state full power conditions.

Comparisons of results obtained by the cylindrical model with results obtained by the detailed HEATING3 representation of the triangular element for the transient response of fuel stick centerline temperature

Table 3-1. Triangular cell model vs cylindrical cell model.

| | Triangular cell (HEATING3) | Cylindrical cell (CORTAP) |
|---|---|---|
| $\Delta T_{FILM}$ (°C) | 229 | 228 |
| $\Delta T_{MODERATOR}$ (°C) | 113* | 114** |
| $\Delta T_{GAP}$ (°C) | 56* | 53 |
| $\Delta T_{FUEL}$ (°C) | 129* | 139 |
| TOTAL (°C) | 527 | 534 |

*Calculated using average fuel and moderator surface temperatures.

**Calculated using a "shape factor" forcing agreement with the triangular cell calculation.

and changes of average fuel and moderator temperatures at an axial location whose axial power peaking factor is unity are shown in Figs. 3.2, 3.3, and 3.4 respectively for the following transients:

1. A 25% step increase in reactor power from full power conditions.
2. A 139°C (250°F) step increase in bulk coolant temperature from full power conditions.
3. A 50% step decrease in film heat transfer coefficient from full power conditions.

It is important that the time response of the changes in average fuel and average moderator temperatures as calculated using the simpler cylindrical cell model agree with those calculated with the more detailed HEATING3 representation because these temperature changes determine the temperature feedback reactivity effects. The good agreement shown in Figs. 3.2, 3.3, and 3.4 provides verification of the approximations used in representing the triangular element with an equivalent cylindrical cell.

In order to determine the transient temperature distribution in the fuel and moderator, the two-dimensional cylindrical cell is divided radially and axially into nodal volumes. Figure 3.5 shows a typical node in an axial segment of the cell between z and $z+\Delta z$. The distance from the fuel stick centerline to the outer surface of node i is denoted $s_i$. The equation for heat conduction in the solid is

$$\nabla\cdot(k\nabla T) + Q = \frac{\partial}{\partial t}(\rho c_p T) \quad . \tag{3.1}$$

Neglecting, for the time being, heat transfer in the axial direction

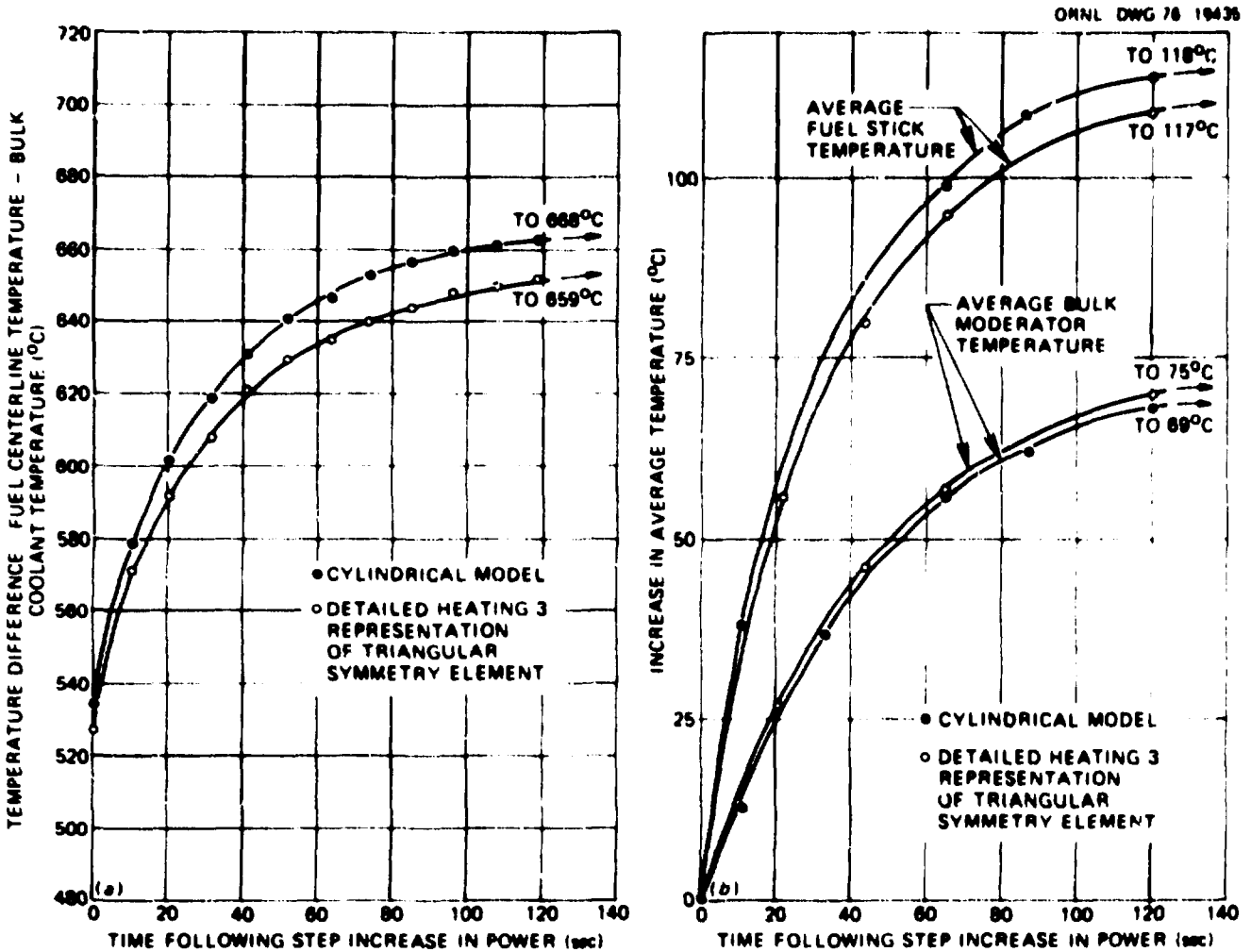


Fig. 3.2. Transient response to step increase in power of 25% — model verification. (a) Fuel centerline temperature; (b) average fuel and moderator temperatures.

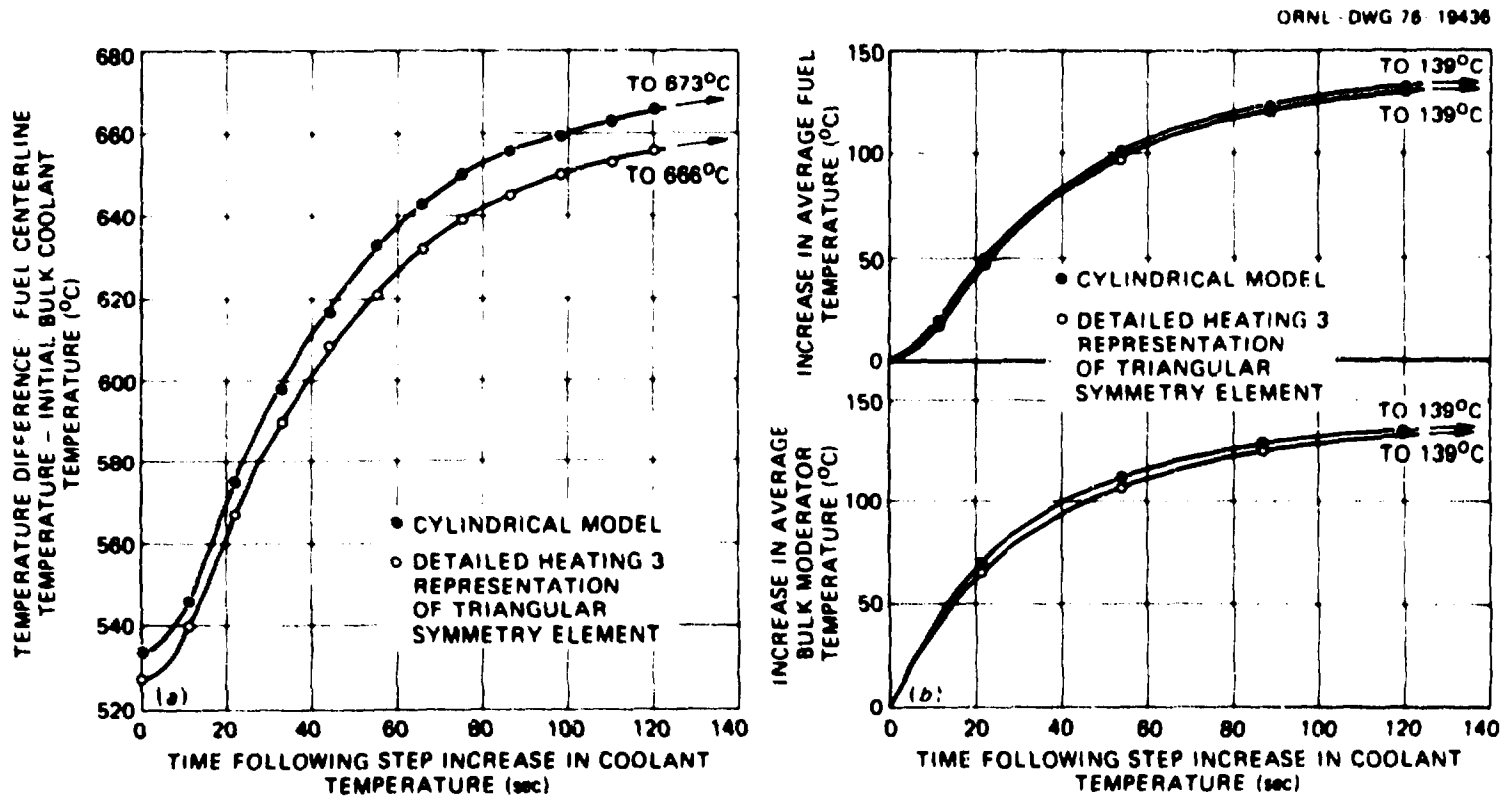


Fig. 3.3. Transient response to step increase in coolant temperature of 139°C (250°F) — model verification. (a) Fuel centerline temperature; (b) average fuel and moderator temperatures.

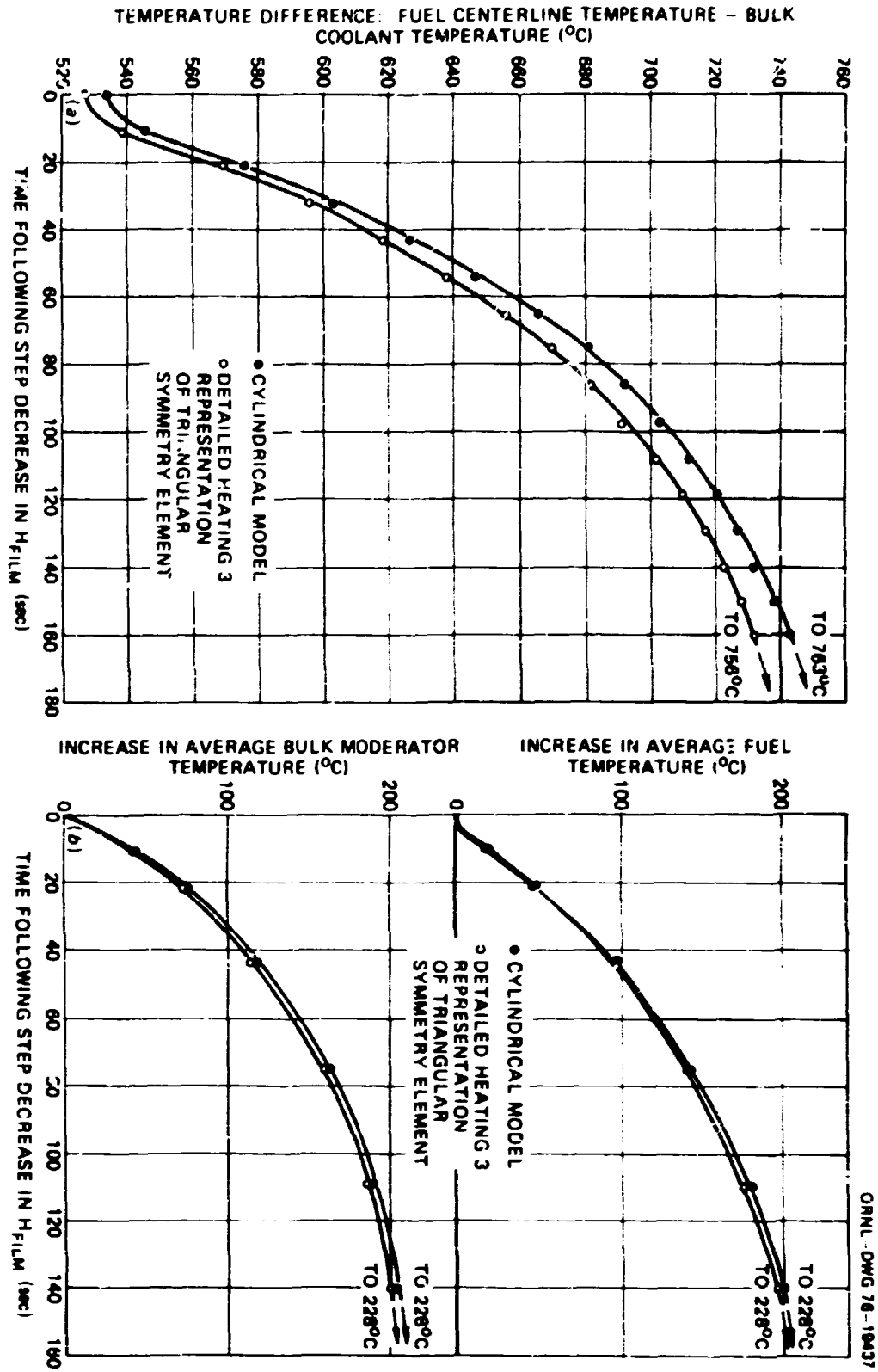


Fig. 3.4. Transient response to step decrease in $h_{film}$ of 50% — model verification. (a) Fuel centerline temperature; (b) average fuel and moderator temperatures.

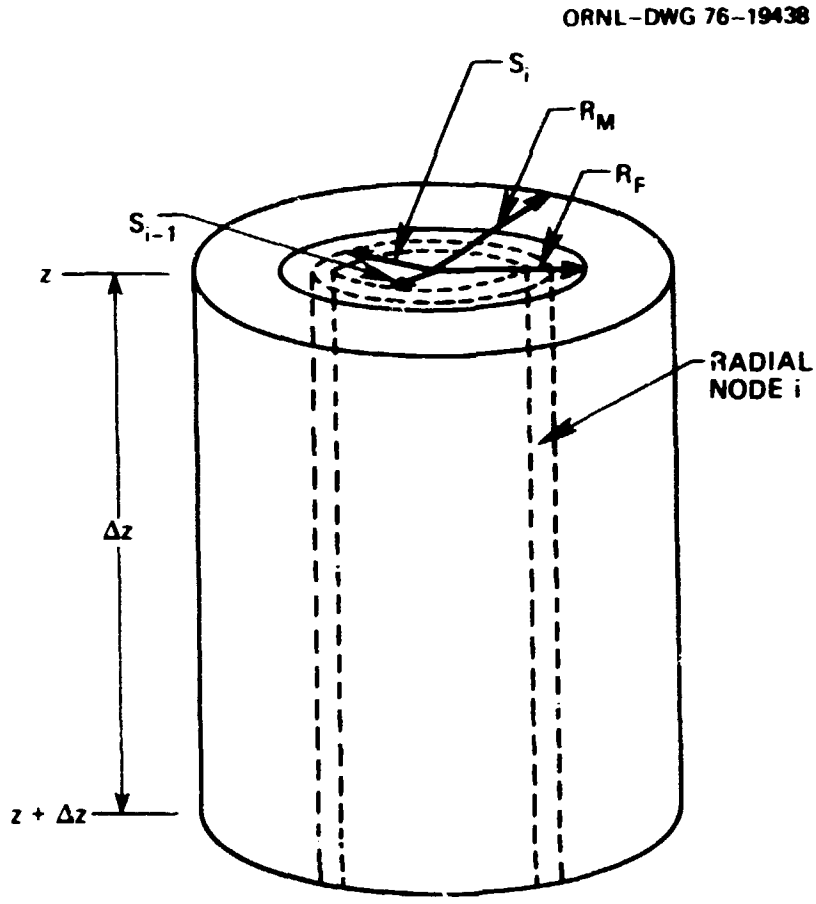


Fig. 3.5. Typical radial node in cylindrical cell.

and integrating this over the volume occupied by node i gives

$$+\int_{\substack{\text{outer surface}\\ \text{of node i}}} k\frac{dT}{dr}(2\pi s_i)\,dz - \int_{\substack{\text{inner surface}\\ \text{of node i}}} k\frac{dT}{dr}(2\pi s_{i-1})\,dz + Q_i V_i = m_i c_p \frac{d\bar{T}_i}{dt}\,, \quad (3.2)$$

where $\bar{T}_i \equiv \frac{1}{V_i}\int_{\substack{\text{volume of}\\ \text{node i}}} T\,dV\,,$

and it has been assumed that both the heat generation rate density Q and the volumetric heat capacity $\rho c_p$ are independent of position within the nodal volume. The first term in the above equation represents the rate of heat transfer from the ith radial nodal volume between z and z+Δz to the i+1st radial nodal volume. Assuming that the rate of heat transfer per unit area from radial node i to radial node i+1, k(dT/dr), is independent of z over the outer surface of node i,

$$\int_{\substack{\text{outer surface}\\ \text{of node i}}} k\frac{dT}{dr}(2\pi s_i)\,dz = \left(k\frac{dT}{dr}\right)\Big|_{s_i}(2\pi s_i)\,\Delta z\,. \quad (3.3)$$

It is customary to define a radial conductance $C_i$ from node i to i+1 such that this rate of heat transfer [Eq. (3.3)] is equal to the product of $C_i$ and the difference in volume average temperatures of the ith and i+1st radial nodal volumes, i.e.,

$$C_i \equiv \frac{\left(k\frac{dT}{dr}\right)\Big|_{s_i}(2\pi s_i)\,\Delta z}{(\bar{T}_{i+1} - \bar{T}_i)}\,. \quad (3.4)$$

It is possible to obtain an expression for $C_i$, defined above, in terms of geometrical quantities and conductivity by considering the steady-state values of $(dT/dr)|_{s_i}$, $\bar{T}_{i+1}$ and $\bar{T}_i$ in Eq. (3.4). In addition to the assumption of uniform heat generation rate density, if it is assumed that the conductivity is independent of radial position, the steady-state radial temperature profile within the ith nodal volume in the fuel stick is parabolic, i.e.,

$$T(r) = T_{\ell} - \frac{Q}{4k_F} r^2 .$$

Substituting for $(dT/dr)|_{s_i}$, $\bar{T}_i$ and $\bar{T}_{i+1}$ in Eq. (3.4) gives

$$C_i = \frac{8k\pi s_i^2 \Delta z}{s_{i+1}^2 - s_{i-1}^2} . \tag{3.5}$$

If equally spaced intervals are used to define the nodal surfaces, i.e., if

$$s_{i+1} = s_i + \Delta r ,$$

and

$$s_{i-1} = s_i - \Delta r ,$$

Eq. (3.5) reduces to the more familiar form

$$C_i = \frac{kA_i}{\Delta r} , \tag{3.6}$$

where

$$A_i = 2\pi s_i \Delta z .$$

Therefore, if the user selects nodal surfaces which have a constant spacing $\Delta r$, the heat transferred radially from the ith nodal volume to the i+1st nodal volume can be written as $(kA_i/\Delta r)(\bar{T}_i - \bar{T}_{i+1})$.

A similar technique is used to determine the conductances in the bulk moderator. However, it is assumed for conservatism that all of the power is generated in the fuel stick and none in the bulk moderator. Therefore the steady-state temperature distribution in the moderator is logarithmic rather than parabolic, i.e.,

$$T(r) = T(R_{IM}) - \frac{QR_F^2}{2k_M} \ln(r/R_{IM}) ,$$

so this form of the temperature profile is used in Eq. (3.4) to obtain conductances for moderator nodes. For transient problems, CORTAP uses conductances obtained by the above technique allowing the conductivity to vary with temperature during the transient.

For conservatism, axial conduction between refueling blocks is allowed only in the moderator portion of the unit cell. CORTAP results indicate that under full flow conditions, axial conduction within the moderator portion decreases peak temperatures in the average powered region at 100% power conditions by only ~2°C out of ~850°C and therefore could be neglected. Also, conservative results are obtained by neglecting axial conduction. However, axial conduction within the moderator portion of the unit cell may be included in CORTAP at the option of the user. The conductance between axial nodes is $C = (kA/\Delta z)$ where A is the area of the axial conduction path, and $\Delta z$ is the axial nodal spacing, taken to be the height of a hexagonal element.

Thus the cylindrical cell is represented by a mesh of nodal points representing the masses associated with concentric rings of the cell. Each node is coupled to neighboring nodes according to the equation of heat conduction in nodal form (j increases in the downward direction):

$$C^r_{i-1,i}\,(T_{i-1,j} - T_{i,j}) + C^r_{i,i+1}\,(T_{i+1,j} - T_{i,j})$$
$$+ C^a_{j,j-1}\,(T_{i,j-1} - T_{i,j}) + C^a_{j,j+1}\,(T_{i,j+1} - T_{i,j})$$
$$+ Q_{i,j}\,V_{i,j} = (\rho c_p V)_{i,j}\,\frac{dT_{i,j}}{dt}\,, \qquad (3.7)$$

where the terms representing axial conduction are omitted for fuel stick nodes, and the term containing $Q_{i,j}$ is omitted for moderator nodes. At the option of the user, a value for radial gap conductance between the fuel stick and moderator may be input and is included in the appropriate conductance terms. The nodal heat generation rate density in the fuel stick is computed from

$$Q_{i,j} = f^z_{i,j} \cdot \frac{n(t)}{n_o} \cdot Q_o\,, \qquad (3.8)$$

where $Q_o$ is the initial average heat generation rate density in the fuel stick, $f^z_{i,j}$ is the input axial peaking factor (assumed constant during transients) and $[n(t)/n_o]$ is the ratio of neutron density at time t to that at time zero. The calculation of n(t) is discussed in section 3-2 of this report.

For the outermost moderator nodes in the cylindrical cell, the second term in the conservation of energy equation [Eq. (3.7)] is replaced by the appropriate expression for heat transfer to the coolant

resulting in

$$C^{r}_{I-1,I}\,(T_{I-1,j} - T_{I,j}) + C'_{j}\,(T_{gas,j} - T_{I,j}) + C^{a}_{j,j-1}\,(T_{I,j-1} - T_{I,j}) + C^{a}_{j,j+1}\,(T_{I,\,j+1} - T_{I,j}) = (\rho c_p V)_{I,j}\,\frac{dT_{I,j}}{dt}\,, \tag{3.9}$$

where I is the number of radial nodes in the representation, and $C'_j$ is the combined conductance from node I,j to the surface of the moderator and the film conductance over the axial length $\Delta z$. The method of relating $T_{gas,j}$ to nodal inlet and outlet gas temperatures is the same as is reported in ORECA-1.[6] The change in helium temperature with distance along the jth axial segment of the cylindrical cell, which is located axially between $(j-1)*\Delta z$ and $j*\Delta z$ is determined by the equation:

$$Wc_{p,He}\,\frac{dT(z')}{dz'} = \frac{C'_j}{\Delta z}\,[T_{I,j} - T(z')]\,, \tag{3.10}$$

where $T(z')$ is the helium temperature at $z'$, and $(j-1)*\Delta z < z' < j*\Delta z$. Solving the equation to obtain the outlet helium temperature from the jth axial segment, $T_{out,j}$, in terms of the segment's inlet gas temperature, $T_{IN,j}$, and the solid temperature, $T_{I,j}$, gives

$$T_{OUT,j} = e^{-(C'_j/Wc_{p,He})}\,T_{IN,j} + \left[1.0 - e^{-(C'_j/Wc_{p,He})}\right]\,T_{I,j}\,. \tag{3.11}$$

Note that this technique assumes that the solid temperature $T_{I,j}$ is constant over the entire length of the node, and that the helium transport time is negligible compared to the thermal time constant of

the solid node. The conservation of energy for the helium associated with the jth axial segment is represented by

$$C_j'(T_{I,j} - T_{gas,j}) = Wc_{p,He}(T_{OUT,j} - T_{IN,j}) \quad . \tag{3.12}$$

The helium flow in each axial node is assumed equal to the channel inlet flow thus neglecting mass storage effects in the helium. Substituting Eq. (3.11) into Eq. (3.12) gives

$$C_j'(T_{gas,j} - T_{I,j}) = Wc_{p,He}\left[1.0 - e^{-(C_j'/Wc_{p,He})}\right] T_{IN,j} - Wc_{p,He}\left[1.0 - e^{-(C_j'/Wc_{p,He})}\right] T_{I,j} \quad . \tag{3.13}$$

However, from Eq. (3.11)

$$T_{IN,j} = T_{OUT,j-1} = e^{-(C_{j-1}'/Wc_{p,He})} T_{IN,j-1} + \left[1.0 - e^{-(C_{j-1}'/Wc_{p,He})}\right] T_{I,j-1} \quad . \tag{3.14}$$

Substituting this into Eq. (3.13) gives

$$C_j'(T_{gas,j} - T_{I,j}) = Wc_{p,He}\left[1.0 - e^{-(C_j'/Wc_{p,He})}\right] e^{-(C_{j-1}'/Wc_{p,He})} T_{IN,j-1} + Wc_{p,He}\left[1.0 - e^{-(C_j'/WC_{p,He})}\right]\left[1.0 - e^{-(C_{j-1}'/WC_{p,He})}\right] T_{I,j-1} - Wc_{p,He}\left[1.0 - e^{-(C_j'/Wc_{p,He})}\right] T_{I,j} \quad . \tag{3.15}$$

When the right-hand side of the above equation is substituted for the second term in the conservation of energy equation for the solid node I,j, i.e., Eq. (3.9), it is obvious that the solid node I,j is coupled to the solid node I,j−1 through heat transfer to the coolant (second term in the above equation) as well as through heat transfer axially through the moderator [third term in Eq. (3.9)]. In like manner, the coupling between the solid nodes I,j and node I,j−2 can be derived by replacing j by j−1 in Eq. (3.14) and substituting for $T_{IN,j-1}$ $(=T_{OUT,j-2})$ in the first term in Eq. (3.15). By using this technique, CORTAP includes the coupling, which is due to heat transfer to the coolant, of each of the outermost moderator nodes to all of the moderator nodes axially above it. This technique also couples each of the outermost moderator nodes to the core inlet temperature and flow rate.

The unit cell in the active fuel is represented in more detail than the upper and lower reflector elements and support block primarily due to the need for accurate fuel and moderator temperatures for the reactivity feedback calculations. The extensions of the unit cell through the upper and lower reflectors are divided into axial nodes, the number of which is determined by the user (generally two or three nodes each). The unit cell in the reflector elements is not divided radially. Therefore the conservation of energy equation for the jth upper or lower reflector node, when axial conduction is considered, is

$$C^R_{a_{j,j-1}}(T^R_{j-1} - T^R_j) + C^R_{a_{j,j+1}}(T^R_{j+1} - T^R_j)$$

$$- Wc_{p,He}\left[1.0 - e^{-(C_j/Wc_{p,He})}\right] T^R_j$$

$$+ Wc_{p,He}\left[1.0 - e^{-(C_j/Wc_{p,He})}\right] T_{IN,j}$$

$$= (\rho c_p V)_j \frac{dT_j^R}{dt} . \qquad (3.16)$$

The coupling of reflector nodes to other solid nodes which transfer heat to the coolant through the $T_{IN,j}$ term in Eq. (3.16) is accomplished in the same manner as has been described for the segment of the unit cell in the active core.

The unit cell is not extended into the core support block (Fig. 2.3) due to the much larger coolant channels in the support block. The support block is modeled with two nodes. The upper node represents one-sixth of the mass of that portion of the block which contains six coolant channels (see Fig. 3.4) and the lower node represents the mass of that portion of the block which contains one large coolant channel. The upper node transfers heat with one-sixth of the region's coolant flow while the lower node transfers heat with the total flow through the region. The heat transfer coefficients and heat transfer areas are based on the appropriate flows and channel dimensions.

CORTAP also models the heat transfer to the coolant flowing through the control rod channels as discussed in Sect. 3.4. The fraction of core power supplied to the coolant in these channels as well as the fraction of total core flow which passes through these channels are assumed to remain equal to their initial steady-state values during the transient. The outlet temperature from these channels and the outlet temperature from the unit cell calculation are weighted by flow rates to obtain a mixed mean gas temperature. This mixed

mean temperature is then used as the inlet temperature for the core support block (see Fig. 2.3).

The film heat transfer correlation used by CORTAP for turbulent flow (Re $\geq$ 4000) is a Dittus-Boelter type correlation:

$$h = (0.02)\,\frac{k}{D}\,(0.88)(Re)^{0.8} ,$$

where 0.88 is approximately the 0.4 power of the Prandtl number. For laminar flow (Re < 2100) CORTAP uses the correlation given in Reference 5.

$$h = (0.656)\,\frac{Gc_{p,He}}{(Re)^{.667}} ,$$

where G is the mass velocity of the helium in lbm/hr-ft$^2$. In the transition region (2100 < Re < 4000) the value of h is obtained by interpolation on the Reynolds number between the value of h(laminar) at Re = 2100 and the value of h(turbulent) at Re = 4000.

The physical properties of helium are represented by

$$\mu = 5.9178 \times 10^{-4}\, T^{0.7} \text{ (lbm/ft-hr)} , \qquad \text{(Ref. 6)}$$

$$k = 1.29 \times 10^{-3}\, T^{0.674} + 8.15 \times 10^{-4}\, (P - 14.69)^{0.28} \text{ (Btu/hr-ft-°R)} , \qquad \text{(Ref. 7)}$$

$$c_{p,He} = 1.2425 \text{ (Btu/lbm-°F)} ,$$

where T is in degrees Rankine, and P is in psia.

The fuel and moderator conductivities may be input to CORTAP through user supplied subroutines as functions of temperature. CORTAP

presently contains subroutines representing the temperature dependence of the volumetric specific heat, $\rho c_p$, for the fuel and moderator based on information presented in Ref. 8:

Fuel

$$\rho c_p = 48.265 - 41.121e^{-T/1000} + 9.6347e^{-2T/1000} \text{ Btu/ft}^3\text{-°F} ,$$

Moderator

$$\rho c_p = 55.605 - 41.059e^{-T/1000} \text{ Btu/ft}^3\text{-°F} ,$$

where T is in °F, and 400°F < T < 2800°F.

The equations representing heat transfer in the fuel and moderator and heat transfer to the coolant [Eqs. (3.7), (3.9) and (3.15)] as well as the equations representing heat transfer from the upper and lower reflector elements to the coolant (3.16) can be written as

$$\underline{A}(\vec{T},W)\vec{T} + \vec{Z}(\vec{Q},W,\vec{T},T_{INLET}) = \frac{d\vec{T}}{dt} , \qquad (3.17)$$

where T is a column vector whose components are $T_1^{UR},\ldots, T_{NUR}^{UR}, T_{1,1}\cdots, T_{I,1}, T_{1,2},\ldots, T_{I,2},\ldots, T_{1,J},\ldots, T_{I,J}, T_1^{LR},\ldots, T_{NLR}^{LR}$. $\underline{A}$ is a matrix whose elements are determined by temperature dependent fuel and moderator conductivities and volumetric specific heats, helium flow rate and film heat transfer coefficients. $\vec{Z}$ is a vector determined by nodal heat generation rate densities $\vec{Q}$, helium flow rate, temperature dependent volumetric specific heat, film heat transfer coefficient and core inlet helium temperature. During the transient, the elements of $\underline{A}$ which are temperature dependent due to the temperature dependence of fuel and moderator conductivities and specific heats and which are flow

rate dependent are recomputed whenever a nodal temperature or the flow rate changes by a given amount, supplied by the user. The components of $\vec{Z}$ are recomputed after each time step.

Assuming that the elements of $\underset{\sim}{A}$ and the components of $\vec{Z}$ can change only at the end of a time step, $\Delta t$, and therefore remain constant during a time step, Eq. (3.17) becomes an inhomogeneous constant coefficient first order differential equation during that time step and its exact incremental solution is

$$\vec{T}(t + \Delta t) = e^{\underset{\sim}{A}\Delta t}\,\vec{T}(t) + (e^{\underset{\sim}{A}\Delta t} - \underset{\sim}{I})\,\underset{\sim}{A}^{-1}\,\vec{Z}(t) \ . \qquad (3.18)$$

The incremental solution $\vec{T}(t + \Delta t)$ is obtained using the MATEXP[9] code. It is important to note that the inverse of $\underset{\sim}{A}$ need not be calculated by MATEXP since

$$(e^{\underset{\sim}{A}\Delta t} - \underset{\sim}{I})\,\underset{\sim}{A}^{-1} = I(\Delta t) + \frac{\underset{\sim}{A}(\Delta t)^2}{2!} + \frac{\underset{\sim}{A}^2(\Delta t)^3}{3!} + \ldots + \frac{\underset{\sim}{A}^{k-1}(\Delta t)^k}{k!} + \ldots . \qquad (3.19)$$

The advantage of the MATEXP integration technique compared to techniques such as Euler integration is that the only approximation is in the choice of the truncation integer, k in the above expansion. Unless the components of $\underset{\sim}{A}$ must be recalculated at $t + \Delta t$ (based on the user input for the allowable change in nodal temperatures and core flow), the solution at $t + 2(\Delta t)$ can be computed without recalculating $(e^{\underset{\sim}{A}\Delta t} - \underset{\sim}{I})\underset{\sim}{A}^{-1}$ since

$$\vec{T}(t + 2\Delta t) = e^{\underset{\sim}{A}\Delta t}\,\vec{T}(t + \Delta t) + (e^{\underset{\sim}{A}\Delta t} - \underset{\sim}{I})\,\underset{\sim}{A}^{-1}\,\vec{Z}(t + \Delta t) \ . \qquad (3.20)$$

## 3.2 Neutron Kinetics Model

The neutron kinetics model used in CORTAP is a point (space independent), one energy group kinetics model with six groups of delayed neutron precursors. The importance of space and spectral effects in HTGR neutron kinetics analyses has been investigated in Reference 10. The conclusion presented is that a point kinetics model with one energy group is sufficiently accurate for slow reactivity changes such as those resulting from fuel or moderator temperature changes and/or slow rod removal transients. The latter transients have reactivity insertion of ~$2.0 at a rate of <2¢/sec. However, for transients such as a fast rod removal transient (rod ejection) with a reactivity insertion of ~$2.0 in 0.1 sec the point kinetics model does not necessarily give conservative results. Transients considered credible in HTGR safety analyses involve reactivity changes of less than one or two cents per second and are therefore within the range of applicability of a space independent, one energy group model.

The point kinetics equations with six groups of delayed neutron precursors are

$$\frac{dC_i}{dt} = -\lambda_i C_i + \frac{nk}{\ell} \beta_i \ , \ i = 1,\ldots, 6 \ , \tag{3.21}$$

$$\frac{dn}{dt} = \frac{n}{\ell}[k(1 - \beta_T) - 1] + \sum_{i=1}^{6} \lambda_i C_i \ , \tag{3.22}$$

where

$C_i$ = delayed neutron precursor concentration for group i,

$\lambda_i \equiv$ delayed neutron decay constant ($sec^{-1}$) for group i,

$\beta_i \equiv$ delayed neutron fraction for group i,

$n \equiv$ neutron density,

$k \equiv$ neutron multiplication factor [$k = (1.0 - \rho)^{-1}$, where $\rho$ is the core excess reactivity],

$\beta_T \equiv \sum_{i=1}^{6} \beta_i$,

$\ell \equiv$ average neutron lifetime from release to loss.

It is convenient to select a unit volume for $C_i$ and n such that for the initial steady-state, n is numerically 1.0. Therefore as n changes during a transient, the reactor power can be obtained by multiplying the initial steady-state power by n(t).

Equations (3.21) and (3.22) can be written as

$$\underset{\sim}{A}(\rho)\vec{X} = \frac{d\vec{X}}{dt} , \tag{3.23}$$

where $\vec{X}$ is a column vector whose components are $C_1, \ldots, C_6$, n. Note that certain components of $\underset{\sim}{A}$ will change with $\rho$. A smaller time step is used for the solution of the neutron kinetics equations than is used for the solution of the heat transfer equations since the response of the reactor power to reactivity changes is much faster than the response of fuel and moderator temperatures to changes in core power. The time steps will be referred to as the neutron kinetics time step, $\Delta t_{NK}$, and the heat transfer time step $\Delta t_{HT}$; $\Delta t_{NK}$ is obtained by dividing $\Delta t_{HT}$ by N where N, supplied by the user, is the integer number of neutron kinetics time steps per heat transfer time step. CORTAP

assumes that $\rho$ is constant over the heat transfer time step, $\Delta t_{HT}$, and changes after each of these time steps.

To begin the iterative coupling procedure between the heat transfer calculation and the neutron kinetics calculation, CORTAP estimates the temperature at each node in the unit cell at $t + (\Delta t_{HT})/2$ given the nodal temperatures at preceeding time steps. Then the corresponding mass average fuel and graphite temperatures $\bar{T}_F$ and $\bar{T}_G$ are obtained as follows:

$$\bar{T}_F = \frac{\sum_{\substack{\text{all fuel} \\ \text{stick nodes}}} T_{i,j} V_{i,j}}{V_{\text{fuel stick}}}, \tag{3.24}$$

$$\bar{T}_G = \frac{\sum_{\substack{\text{all moder-} \\ \text{ator nodes}}} T_{i,j} [\rho_G^{(M)} V_{i,j}] + \sum_{\substack{\text{all fuel} \\ \text{stick nodes}}} T_{i,j} [\rho_G^{(F)} V_{i,j}] f}{\rho_G^{(M)} V_{\text{moderator}} + \rho_G^{(F)} f V_{\text{fuel stick}}},$$

where

$T_{i,j}$ = nodal average temperature from t to $t + \Delta t_{HT}$ for node i,j,

$V_{i,j}$ = volume of node i,j,

$\rho_G^{(M)}$ = density of graphite in the moderator,

$\rho_G^{(F)}$ = density of graphite in the fuel stick,

f = volume fraction of graphite in fuel stick.

The above formulation for $\bar{T}_G$ allows the faster response of the temperature of the graphite in the fuel stick, as opposed to the graphite in

the bulk moderator, to be accounted for in the reactivity feedback calculation.

Next, the reactivity feedback due to temperature changes is determined from

$$\rho_{feedback} = \int_{\bar{T}_{F,Ref}}^{\bar{T}_F} \alpha_F(T_F)\, dT_F + \int_{\bar{T}_{G,Ref}}^{\bar{T}_G} \alpha_M(T_M)\, dT_M \,, \qquad (3.25)$$

where

$\alpha_F$ ≡ the temperature dependent fuel temperature coefficient of reactivity ($\Delta\rho/°F$),

$\alpha_M$ ≡ the temperature dependent moderator temperature coefficient of reactivity ($\Delta\rho/°F$),

$\bar{T}_{F,Ref}$ ≡ the reference fuel temperature, i.e., when $\rho = 0.0$, °F,

$\bar{T}_{G,Ref}$ ≡ the reference graphite temperature, i.e., when $\rho = 0.0$, °F.

The temperature dependent coefficients of reactivity are determined by user-supplied subroutines. The total reactivity is determined from

$$\rho = \rho_{feedback} + \Delta\rho_{rod} \,, \qquad (3.26)$$

where

$\Delta\rho_{rod}$ ≡ the change in reactivity due to control rod motion.

Since the value of $\rho$ used in Eq. (3.23) is assumed to be constant from t to $t + \Delta t_{HT}$, that equation can be considered to be a constant coefficient, homogeneous first order differential equation for the N neutron kinetics time steps from t to $t + \Delta t_{HT}$. Thus the exact solution is

$$\vec{X}(t + i\Delta t_{NK}) = e^{A\Delta t_{NK}} \vec{X}[t + (i - 1)\Delta t_{NK}] \text{ , where } (i=1,\ldots, N). \tag{3.27}$$

The solution is obtained using the MATEXP[9] code. Now that $n(t + i\Delta t_{NK})$ is known for i=1,..., N, CORTAP determines the average neutron density, denoted as $\bar{n}$, from t to $t + \Delta t_{HT}$ from

$$\bar{n} = \frac{1}{\Delta t_{HT}} \int_{t}^{t+\Delta t_{HT}} n(t)dt \ . \tag{3.28}$$

This value of $\bar{n}$ is then used to determine nodal heat generation rate densities $Q_{i,j}$ from

$$Q_{i,j} = Q_{i,j,o}\, \bar{n}/n_o \ .$$

That is, the terms in the "constant over $\Delta t_{HT}$" $\vec{Z}$ vector of Eq. (3.18) which depend on nodal heat generation rate densities are determined by the average values of these nodal heat generation rate densities over the time step $\Delta t_{HT}$. The heat transfer equations are now solved to yield nodal temperatures at time $t + \Delta t_{HT}$ which are then used to improve the estimate of nodal temperatures at $t + (\Delta t_{HT})/2$ upon which the reactivity feedback calculation is based. The entire procedure is then repeated until convergence on $\rho_{feedback}$ is achieved. Convergence is rapid because fuel and moderator temperatures change slowly due to the large heat capacity of the core. The iteration procedure is outlined in Fig. 3.6.

Following a reactor trip, the neutron kinetics calculations are omitted, and the nodal heat generation rate densities, $Q_{i,j}$, are determined from

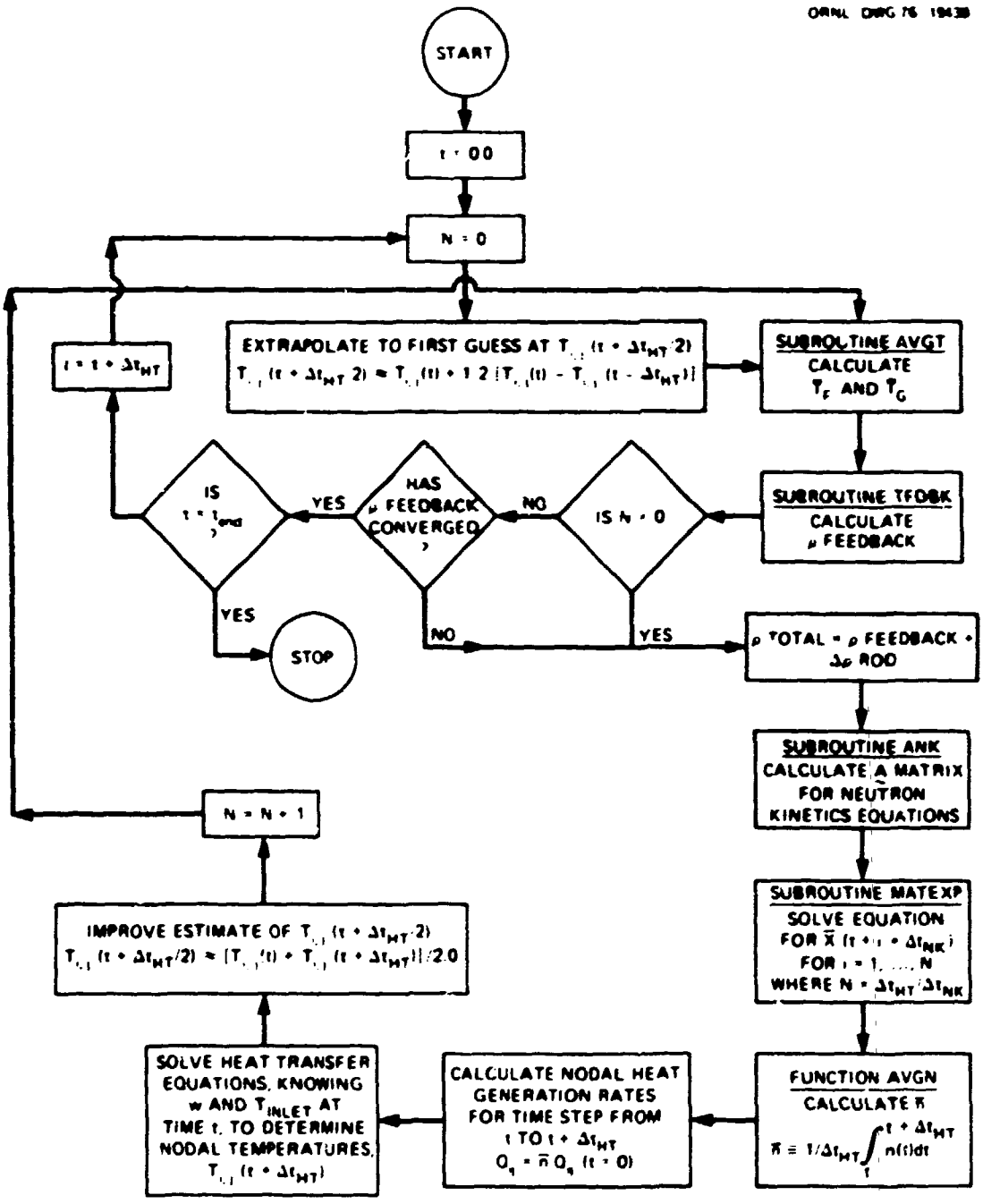


Fig. 3.6. CORTAP iteration procedure for determining feedback reactivity.

$$Q_{i,j} = Q_{i,j,o} \cdot \frac{1}{\Delta t_{HT}} \int_{t}^{t+\Delta t_{HT}} f(t')dt' \,, \qquad (3.29)$$

where f(t) is an expression for power decay following a scram:[11]

$$f(t) = 0.128(t + 3.796 \times 10^{-4})^{-.261} \,, \qquad (3.30)$$

where t is in seconds.

### 3.3 Heat Transfer in Control Rod Channels and Side Reflector

The heat transfer to the helium flowing through the control rod channels and to the helium flowing through the side reflectors is not treated in as much detail as the heat transfer to the helium flowing through the coolant channels associated with the unit cell. Nor does the heat transfer in the control rod channels and the side reflector have any effect on the neutron kinetics calculations since the reactivity feedback effects are based only on the fuel and graphite temperatures determined by the unit cell calculation. The effects of heat transfer in the control rod channels and side reflectors are included primarily to determine a core mixed mean outlet gas temperature. The control rod channel heat transfer calculations are discussed below; the side reflector calculations are done in a similar manner.

The fraction of total core power supplied to the mass of graphite which transfers heat with the control rod channels and the fraction of total core flow which passes through these channels are assumed to remain equal to their initial steady-state values during the transient. This

avoids the difficulty of defining an equivalent conductance from an average fuel stick to the control rod channel in order to determine the heat deposited in the coolant. The mass of solid transferring heat to the coolant flowing through the control rod channels is divided axially into nodes. The temperatures $T_{S,j}$ of the solid axial nodes are determined from

$$Mc_j \frac{dT_{S,j}}{dt} = h_j A_j (T_{b,j} - T_{S,j}) + Q_j \ , \tag{3.31}$$

where $T_{b,j}$ is the bulk temperature of the coolant associated with the jth axial solid node. Integrating from t to $t + \Delta t_{HT}$ and assuming that

$$\int_t^{t+\Delta t_{HT}} T_{S,j}(t')dt' = \frac{1}{2}[T_{S,j}(t + \Delta t_{HT}) + T_{S,j}(t)] \, \Delta t_{HT} \ , \tag{3.32}$$

gives

$$Mc_j [T_{S,j}(t + \Delta t_{HT}) - T_{S,j}(t)]$$

$$= h_j A_j \Delta t_{HT} \left\{ \bar{T}_{b,j} - \frac{[T_{S,j}(t + \Delta t_{HT}) + T_{S,j}(t)]}{2} \right\} + (\Delta t_{HT}) \, \bar{Q}_j \ , \tag{3.33}$$

where

$$\bar{T}_{b,j} = \frac{1}{\Delta t_{HT}} \int_t^{t+\Delta t_{HT}} T_{b,j} dt' \ ,$$

with

$$\bar{Q}_j = \bar{Q}_j(t = 0) \cdot \bar{n}/n_o \ ,$$

or, if the reactor has been tripped

$$\bar{Q}_j = \bar{Q}_j(t = 0)\ \frac{1}{\Delta t_{HT}} \int_t^{t+\Delta t_{HT}} f(t')dt' \ ,$$

with $f(t')$ determined from Eq. (3.30). Using

$$Wc_{p,He}(T_{OUT,j} - T_{IN,j}) = h_j A_j (T_{S,j} - T_{b,j}) \ , \qquad (3.34)$$

and

$$T_{b,j} = 0.5(T_{OUT,j} + T_{IN,j}) \ , \qquad (3.35)$$

Eq. (3.33) can be solved for $T_{S,j}(t + \Delta t_{HT})$ in terms of $T_{S,j}(t)$, $\bar{Q}_j$ and $\bar{T}_{IN,j}$. Due to the assumption [Eq. (3.35)] that $T_{b,j}$ is the arithmetic average of $T_{IN,j}$ and $T_{OUT,j}$, the user must be careful to select the number of axial nodes representing the graphite associated with the control rod channels or with the side reflector such that $(hA/Wc_{p,He}) < 2$ is satisfied.[12] If the core inlet temperature, $T_{INLET}$ vs time from t to $t + \Delta t_{HT}$ is known, it is possible to determine $\bar{T}_{IN,1}$. If $T_{INLET}$ is known only at time t, $\bar{T}_{IN,1}$ is set equal to $T_{INLET}$. Then $T_{S,1}(t + \Delta t_{HT})$ and $T_{OUT,1}(t + \Delta t_{HT})$ can be calculated. The calculation then proceeds to the second axial node with $\bar{T}_{IN,2}$ being determined from $T_{OUT,1}(t)$ and $T_{OUT,1}(t + \Delta t_{HT})$. Once $T_{OUT}(t + \Delta t_{HT})$ from the control rod channel is known, the inlet helium temperature to the core support block is determined by appropriately mixing this helium with the helium exiting the smaller diameter coolant channels through the active fuel as determined from the unit cell calculation. A similar calculation to that described above is done to determine the outlet temperature from the core support block. Helium with this outlet temperature is then appropriately mixed

with the helium exiting the side reflector to determine the core mixed mean outlet helium temperature.

### 3.4 Comparison with General Atomic Company Calculations

As a first step in the verification of CORTAP, comparisons were made with General Atomic Company (GAC) results. Figure 3.7 shows steady-state axial temperature profiles computed by CORTAP and by GAC as reported in The Preliminary Safety Analysis Report,[13] for an average fuel region in the Summit reactor (Delmarva Power Co.) at 100% power. Each of the circles in Fig. 3.7 representing the fuel centerline and maximum graphite temperatures calculated by CORTAP should be considered as representing averages over each one-eighth of the active core height. Considering this, the results compare favorably with those reported by GAC.

Results for both steady-state and transient conditions obtained using CORTAP to simulate the Fort St. Vrain reactor core have been compared to results obtained at ORNL using BLØØST-5,[14] a CAC coupled heat transfer, neutron kinetics code. Both codes model the core with a single average channel and represent the neutron kinetics with the space-independent model. Therefore, they can be expected to give quite similar results. The steady-state comparison was made for 100% power conditions. Although a much finer mesh approximation was used for the BLØØST-5 calculations, for the steady-state the two codes agreed to within less than 6°C on fuel centerline temperatures in the average fuel stick. (Fuel centerline temperatures range from ~566°C to ~900°C in the average fuel column, depending on the axial location.) The

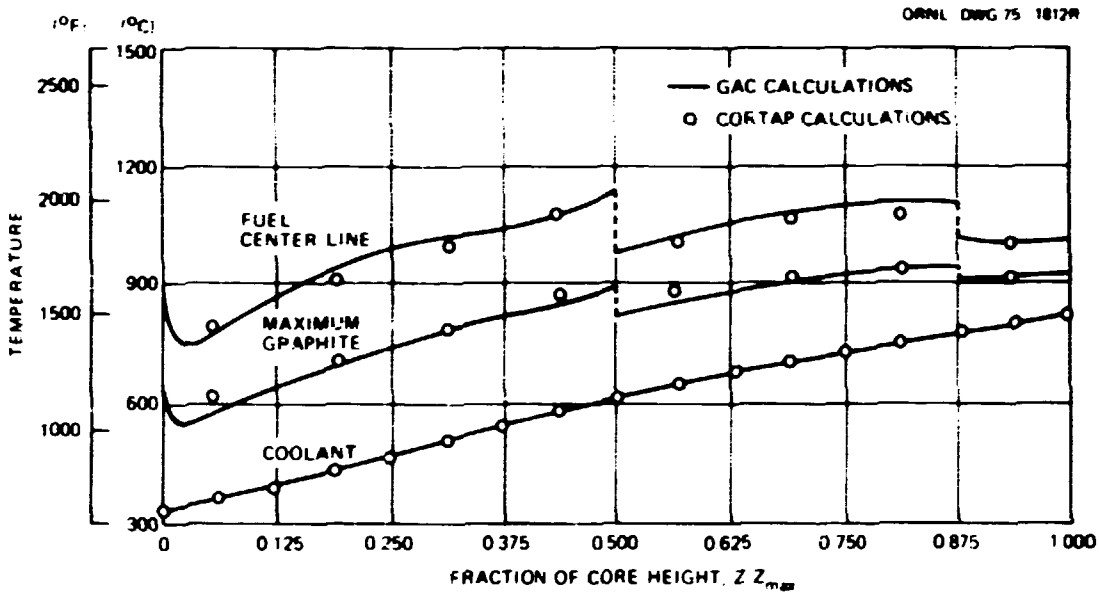


Fig. 3.7. Comparison of GAC and ORNL steady-state axial core temperature distribution.

transient case considered for the BLAST-5 comparison was a one cent step increase in reactivity at full power conditions. "Beginning-of-cycle-one" neutron kinetics parameters and reactivity coefficients were used. Figures 3.8-a, b, and c compare the normalized power, core excess reactivity, and average channel outlet temperature obtained by the two codes. As can be seen, the agreement is quite favorable. The above comparisons provide an analytical verification of CORTAP. Further verification of CORTAP can be achieved when results of test on the FSV reactor become available.

## 4. FUTURE APPLICATIONS OF CORTAP

In addition to transient analyses of postulated accidents performed for both ERDA and NRC, CORTAP has been coupled with codes which simulate the HTGR helium circulator and circulator turbine, reheater and steam generator (BLAST[15]) and the turbine generator plant resulting in the ORTAP code. ORTAP is being used initially to analyze the effect on the core of the postulated system transients, outlined in reference 16, for the Fort St. Vrain reactor.

Because CORTAP uses a cylindrical cell model, it could be used as a coupled heat transfer-neutron kinetics simulation of the GCFR core, or any other core involving cylindrical fuel pins, with only minor modification.

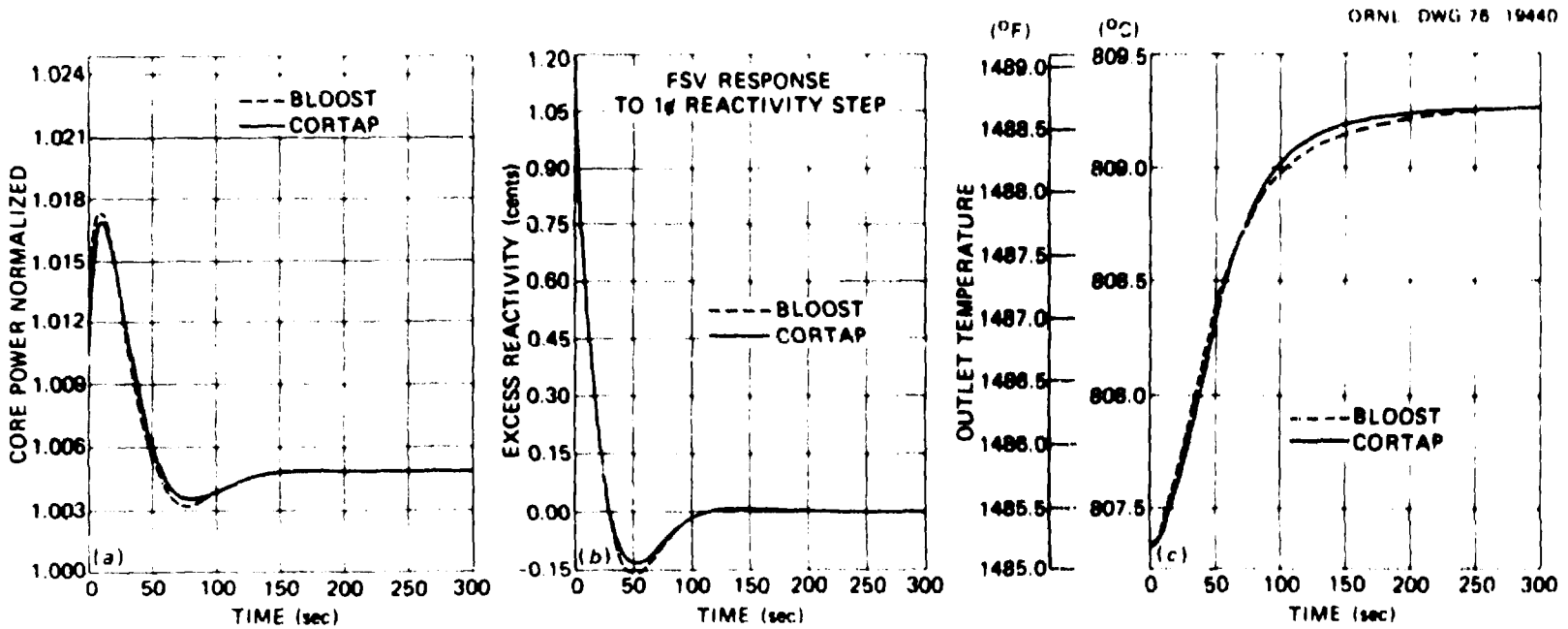


Fig. 3.8. Comparison of response of core normalized power (a) core excess reactivity (b), and coolant outlet temperature (c) to a + 1¢ step change in reactivity.

## 5. REFERENCES


1. A. Bardia and R. C. Potter, TAP: A Program for Analysis of HTGR Nuclear Steam Supply System Performance Transients, GA-A13248, January 30, 1976.
2. J. P. Sanders, et al., Evaluation of Thermal Response in Fort St. Vrain Reactor Primary System to a Design Basis Depressurization Accident Followed by Cooling with Two Pelton Wheel Drives Operating at 7000 rpm, ORNL-TM-5140 (December 1975).
3. W. D. Turner and M. Siman-Tov, HEATING3 - An IBM 360 Heat Conduction Program, ORNL-TM-3208 (February 1971).
4. S. J. Ball, ORECA-1: A Digital Computer Code for Simulating the Dynamics of HTGR Cores for Emergency Cooling Analysis, ORNL/TM-5159 (April 1976).
5. Letter, P. R. Kasten to R. A. Clark, Chief of Gas Cooled Reactor Branch, Directorate of Licensing, USAEC, Subject: "HTGR Safety Studies Progress Report for the Period Ending Dec. 31, 1973," (January 30, 1974).
6. H. Petersen, Risö Report No. 224, September 1970.
7. J. R. Tallackson, The Thermal Transport Properties of Helium, Helium-Air Mixtures, Water and Tubing Steel Used in the CACHE Program to Compute HTGR Auxiliary Heat Exchanger Performance, ORNL-TM-4931.
8. Letter, D. S. Duncan, Manager, Plant Licensing Branch, GAC to R. A. Clark, Chief of Gas Cooled Reactors Branch, Directorate of Licensing, USAEC, Subject: "Answers to Request for Additional Information No. 1

on Licensing Topical Report No. 1 (GA-LTR-1)," "An Analysis of HTGR Core Cooling Capability," (February 6, 1974).

9. S. J. Ball and R. K. Adams, "MATEXP," A General Purpose Digital Computer Program for Solving Ordinary Differential Equations by the Matrix Exponential Method, ORNL-TM-1933, (August 1967).

10. R. Brogli and R. Froehlich, "Space and Spectrum Effects for Rod Removal Transients in an HTGR," Trans. American Nuclear Society 13, (June-July 1970).

11. H. W. Chi and G. J. Malek, Description of the Reactor Emergency Cooling Analysis Code, RECA, GA-10273 (August 19, 1970).

12. S. J. Ball, "Approximate Models for Distributed-Parameter Heat-Transfer Systems," ISA Transactions, (January 1964).

13. Delmarva Power & Light Co., Summit Power Station, Preliminary Safety Analysis Report (1973-74).

14. M. Merrill and M. Troost, "BLØØST-5: A Combined Reactor Kinetics-Heat Transfer Code," GAMD-6644, (August 1965).

15. R. A. Hedrick and J. C. Cleveland, BLAST: A Digital Computer Program for the Dynamic Simulation of the High Temperature Gas Cooled Reactor Reheater-Steam Generator Module, ORNL/NUREG/TM-38, (August 1976).

16. Letter, A. R. Rosztoczy, Chief, Analysis Branch, Division of Systems Safety, USNRC to R. D. Schamberger, Chief, Experimental Gas Cooled Reactor Safety Research Branch, DRSR, USNRC, Subject: "Definition of Transients for Fort St. Vrain," June 2, 1976.

# APPENDIX

## CORTAP INPUT INSTRUCTIONS AND SAMPLE INPUT LISTING

The input instructions and a sample input listing for a Fort St. Vrain simulation with CORTAP follow. The instructions can be more easily understood by referring to the sample input listing.

Card No. 1 (FORMAT 20A4)

Title card.

Card No. 2 (FORMAT 10X, 3I5)

IPOWER - Flag indicating how core power will be determined.

1 = core power vs time information is supplied by user.

Note: A subroutine is available which allows the user to supply power, flow rate and inlet temperature vs time for "hot stick" calculations. For these calculations the power vs time function should be obtained from an average fuel stick calculation with IPOWER = 0.

0 = core power is calculated from neutron kinetics equations or from decay heat curve depending on whether the reactor has been tripped or not.

IROD - A parameter specifying whether control rod motion will introduce reactivity during the transient or not.

0 = no control rod motion.

1 = control rod motion.

If IROD = 1, the user must supply a subroutine to be called from the main program specifying the reactivity

BLANK PAGE

change due to rod motion as a function of time.

Note: If IPOWER = 1, this option is ignored.

IPPNCH - Flag indicating whether power vs time is to be punched on cards for a subsequent "hot stick" calculation.

1 = punch.

0 = do not punch.

Card No. 3 (FORMAT 10X, 5D10.4)

CORPWR - Initial thermal power level in MW.

FPC - Fraction of total thermal power deposited to coolant flowing through coolant channels in active core.

FPSR - Fraction of total thermal power deposited to coolant flowing through side reflector elements.

FPGT - Fraction of total thermal power deposited to coolant flowing through control rod channels.

FPAFS - Fraction of FPC*CORPWR that is generated in the entire axial length of an average fuel stick column.

Card No. 4 (FORMAT 10X, 5D10.4)

FLOW - Initial total core flow (lbm/hr). If total core flow is time dependent, the user should provide a subroutine to be called from the main program which expresses this time dependence.

FFC - The fraction of the total core flow which flows through coolant channels.

FFSR - The fraction of the total core flow which flows through side reflector.

FFGT - The fraction of the total core flow which flows through control rod channels.

FFACC - The fraction of FFC*FLØW which flows through the average coolant channel.

Card No. 5 (FORMAT 10X, 7I5)

JMAX - Number of axial nodes in the active fuel portion of the unit cell.

NF - Number of radial nodes in the fuel stick.

NM - Number of radial nodes in the moderator.

NATR - Number of axial nodes in top reflector.

NABR - Number of axial nodes in bottom reflector.

NGTN - Number of axial nodes representing mass of graphite transferring heat with coolant flowing through a control rod channel.

NSRN - Number of axial nodes in side reflector.

The restrictions are

$$JMAX*(NF+NM) + NATR + NABR \leq 60$$

$$NGTN \leq 8$$

$$NSRN \leq 8$$

Card No. 6 (FORMAT 10X, 2D10.4)

RPF - Radial power peaking factor. If RPF = 1.0, calculation is for average stick. If RPF = maximum radial peaking factor, a "hot stick" calculation will be performed. Note: For this case, the user should use IPOWER = 1 on card 2 and supply power vs time from an average fuel stick calculation.

RFF - Radial flow factor for coolant in cell being simulated.

Card No. 7 (FORMAT 10X, 4D10.4)

RF - Radius of the fuel stick (in.).

GAP - Width of gap between fuel stick and moderator (in.).

Note: This is used to determine gap conductance, $C_{gap} = (h_{gap} * A)/GAP$.

RM - Outer radius of graphite annulus in cylindrical cell simulation (in.). This should be calculated to conserve the graphite volume in the triangular cell.

HEIGHT - Active core height (in.).

Card(s) No. 8 (FORMAT 10X, 7D10.4)

AXZ(J), J=1, JMAX - The axial location of the centers of the nodal volumes in the active fuel (in.). By definition z=0 at the top of the active fuel column increasing in the downward direction.

Card(s) No. 9 (FORMAT 10X, 7D10.4)

R(I), I=1, IMAX where IMAX = NF + NM.

Distances from the fuel stick centerline to the radial surfaces of the nodes in the cylindrical representation of the unit triangular cell (in.).

Card No. 10 (FORMAT 10X, 2D10.4, 2I5)

SRH - The height of the side reflector (in.).

SRAREA - The cross-sectional area of a side reflector symmetry element ($in.^2$).

NCCSRE - The number of coolant channels in a side reflector element.

NSRC - The number of side reflector columns.

Card No. 11 (FORMAT 10X, D10.4)

TRT - The thickness of the top reflector (in.).

Card No. 12 (FORMAT 10X, D10.4, I5)

HDGT - The hydraulic diameter of the control rod channels (ft).

NGT - The number of control rod channels.

Card No. 13 (FORMAT 10X, D10.4)

VOLGTT - The total volume of graphite which the user allows to transfer heat with the average control rod channel ($in.^3$). This is used for heat capacity effects.

Card No. 14 (FORMAT 10X, 6D10.4)

RHOFUL - The density of the fuel stick ($lbm/ft^3$), See note.

RHOMOD - The density of the bulk moderator ($lbm/ft^3$). See note.

DENRAT - The ratio of the density of the graphite in the fuel stick to the density of the graphite in the bulk moderator.

F - The volume fraction of the graphite in the fuel stick.

RHOGT - The density of the graphite in the mass transferring heat with coolant flowing through the average control rod channel ($lbm/ft^3$). See note.

RHOSR - The density of the side reflector ($lbm/ft^3$). See note.

NOTE: If the temperature dependent heat capacities in subroutines CPFUEL and CPMOD have units of $Btu/ft^3-°F$, the corresponding "densities" (RHØFUL and RHØMØD) should be input as 1.0. If it is desired to account for the larger graphite to fuel stick mass ratio in the refueling region than in the unit cell, the value input for RHOMOD can be used to account for this.

Card No. 15 (FORMAT 10X, 3D10.4, I5)

BRT - The thickness of the bottom reflector (in.).

BRCHAN - The radius of the coolant channel through the bottom reflector (in.).

ABR - The cross-sectional area of the triangular graphite symmetry element in the bottom reflector ($in.^2$).

NCCELM - The number of coolant channels in the active fuel feeding the bottom reflector channel.

Card(s) No. 16 (FORMAT 10X, 7D10.4)

AXPF(J), J=1, JMAX - The axial power peaking factors for the fuel stick.

Card No. 17 (FORMAT 10X, 3D10.4, I5)

TZERO - Problem beginning time (sec).

TFINAL - Problem end time (sec).

DELTTH - The time step for heat transfer calculations (sec).

NINC - The number of neutron kinetics time steps per heat transfer time step.

Card No. 18 (FORMAT 10X, 4D10.4, 3I5)

DELTMP - The maximum amount that any nodal temperature can change without recalculating the components of the $\underline{A}$ matrix [Eq. (3.18)] (°F). Some experimentation on this parameter by the user is advisable to minimize computer time while maintaining sufficient accuracy. In general, the "weaker" the temperature dependence of fuel and moderator conductivities and specific heats, the larger this value can be.

DLMDOT - The maximum amount that the total core flow rate can change without recalculating the components of the $\underset{\sim}{A}$ matrix [Eq. (3.17)] (lbm/hr). No single value for this parameter can be recommended since the value which would maintain sufficient accuracy while keeping computer time as low as possible depends on how low the core flow becomes in any given transient. Some experimentation on this parameter by the user is advisable to minimize computer time while maintaining sufficient accuracy.

DTOPTT - Should be input greater than DELTTH (Card 17) unless user desires printout of the $\underset{\sim}{A}$ matrix, the $e^{\underset{\sim}{A}\Delta t_{HT}}$ matrix and the $[e^{\underset{\sim}{A}\Delta t_{HT}} - \underset{\sim}{I}]\underset{\sim}{A}^{-1}$ matrix for Eq. (3.18) calculated by MATEXP (sec).

DTOPTN - Should be input greater than DELTTH unless user desires printout of the $\underset{\sim}{A}$ matrix and the $e^{\underset{\sim}{A}\Delta t_{NK}}$ matrix for Eq. (3.27) calculated by MATEXP (sec).

NOUPDT - Flag for updating the $\underset{\sim}{A}$ matrix [Eq. (3.17)] due to temperature dependence of its elements after each iteration on feedback reactivity.

= 0 update $\underset{\sim}{A}$.

= 1 do not update $\underset{\sim}{A}$.

This option is somewhat obsolete and NOUPDT = 1 is recommended. If NOUPDT = 0 is used, problem execution time is greatly increased with essentially no improvement in accuracy.

NPT - Number of heat transfer time steps between printouts.

IPUNCH - Flag for punching nodal temperatures and coolant temperatures existing at end of execution.

= 1 punch.

= 0 do not punch.

Card No. 19 (FORMAT 10X, 3D10.4)

HGAP - The heat transfer coefficient of the gap between the fuel and moderator (Btu/hr-ft$^2$-°F).

D - The hydraulic diameter of a coolant channel (ft).

TINLET - The initial inlet temperature (°F). Note: If inlet gas temperature is time dependent, the user should provide a subroutine to be called from the main program which expresses the time dependence.

Card No. 20 (FORMAT 10X, I5, 2D10.4)

NG - Number of groups of delayed neutron precursors.

EPSLON - The convergence criteria for reactivity feedback. Recommend 1.0D-9.

RLSTAR - The average neutron lifetime [$\ell$ in Eqs. (3.21) and (3.22)] from release to loss (sec).

Card No. 21 (FORMAT 10X, 7D10.4)

BETA(I), I=1, NG - The delayed neutron fraction for precursor group I.

Card No. 22 (FORMAT 10X, 7D10.4)

RLMBDA(I), I=1,..., NG - The decay constant for precursor group I (sec$^{-1}$).

Card No. 23 (FORMAT 10X, 2D10.4)

TMREF - The reference graphite temperature for reactivity feedback [Eq. (3.25)] (°F).

TFREF - The reference fuel stick temperature for reactivity feedback [Eq. (3.25)] (°F).

Card No. 24 (FORMAT 10X, D10.4, 5X, I5, D10.4)

This card contains information pertaining to the MATEXP integration technique. For further details see reference 9.

P - Precision of $e^{\underline{A}\Delta t}$ and $[e^{\underline{A}\Delta t} - \underline{I}]\underline{A}^{-1}$. Recommend $10^{-6}$ or less.

ITMAX - Maximum number of terms in series approximation of $e^{\underline{A}\Delta t}$. The value of 64 for this parameter is sufficient.

VAR - Maximum allowable value of largest coefficient matrix element $*\Delta t$ (Recommend VAR=1.0).

Cards No. 25 (FORMAT 10X, 7D10.4)

XICT(I), I=1,..., NET, where NET = IMAX*JMAX + NABR + NATR

Initial nodal temperatures in upper reflector, active fuel cell and lower reflector (°F). If a steady-state solution is desired, these are reasonable guesses at the nodal temperatures; if a transient calculation is to be performed, these are the results of a previous steady-state calculation with IPUNCH = 1.

Cards No. 26 (FORMAT 10X, 7D10.4)

TBULK(J), J=1, JEND where JEND = NATR + JMAX + NABR

Gas temperatures corresponding to each solid nodal increment in the upper reflector, the active fuel cell and the

lower reflector. These are the temperatures from which the temperature dependent helium transport properties are obtained (°F).

RESPONSE TO FLOW REDUCTION FROM 100 % POWER CONDITIONS (FORT ST VRAIN)

| | | | | | | | |
|---|---|---|---|---|---|---|---|
| | 0 0 0 | | | | | | |
| | 842.0 | .9415 | 0.01090 | .047 | .20685E-4 | | |
| USER MUST | 3.39E+6 | .87316 | 0.0354 | .09145 | 0.4137E-4 | | |
| SUPPLY | 6 4 | 2 3 | 3 4 | 8 | | | |
| SUBROUTINE | 1.00 | 1.00 | | | | | |
| IN MAIN | 0.245 | 0.005 | 0.42143 | 177.0 | | | |
| EXPRESSING | 14.75 | 44.25 | 73.75 | 103.25 | 132.75 | 162.25 | |
| INLET FLOW | .06125 | .1225 | .18375 | .245 | .33635 | .42143 | |
| VS. TIME | 270.6 | 0.56 | 108 66 | | | | |
| | 46.8 | | | | | | |
| | 0.3333 | 74 | | | | | |
| | 4220.0 | | | | | | |
| | 1.0 | 1.0 | 1.0 | 0.6 | 1.0 | 1.0 | |
| | 46.8 | 0.309 | 1.1227 | 1 | | | |
| | 0.74 | 1.08 | 1.35 | 1.15 | 0.99 | 0.69 | |
| | 0.0 | 235. | 0.1 | 20 | | | |
| | 20. | 1000. | 1000000. | 1000000. | 1 50 | 1 | |
| | 400.0 | .0515 | 748.0 | | | | |
| END OF EQ. | 6 | 1.00-10 | 3.410-4 | | | | |
| CYCLE | 0.000222 | .001099 | .000961 | .001619 | .00043 | .000179 | |
| NEUTRON | 0.01251 | 0.03164 | 0.1199 | 0.3068 | 1.135 | 2.859 | |
| KINETICS | 1390.1723 | 1506.7677 | | | | | |
| DATA | 1.00-6 | 64 | 1.0 | | | | |
| INITIAL | 748.0000 | 748.0000 | 748.0000 | 1104.8443 | 1097.8612 | 1083.8950 | 1062.9453 |
| NODAL | 979.8318 | 953.7352 | 1358.9014 | 1348.7220 | 1328.3532 | 1297.8249 | 1176.6718 |
| TEMPS ARE | 1138.6314 | 1620.7499 | 1608.0339 | 1582.6022 | 1544.4552 | 1393.1200 | 1365.6028 |
| FOR FLOW | 1688.9788 | 1678.1465 | 1656.4821 | 1623.9861 | 1495.0702 | 1454.5923 | 1751.4288 |
| OF | 1742.1021 | 1723.4489 | 1695.4697 | 1584.4726 | 1549.6210 | 1727.7276 | 1721.2248 |
| 3.39E+6 | 1708.2193 | 1688.7113 | 1611.3205 | 1587.0208 | 1482.6854 | 1482.6854 | 1482.6854 |
| LBM/HR | 748.0000 | 748.0000 | 748.0000 | 793.3721 | 904.8824 | 1053.6351 | 1206.6256 |
| | 1337.5954 | 1440.4373 | 1482.6854 | 1482.6854 | 1482.6854 | | |

## ACKNOWLEDGMENTS

Sincere thanks is expressed to S. J. Ball for his discussions with the author concerning various modeling techniques during the development of CORTAP and to Paula Renfro for her patience in preparing this report.